Article

Nanoliter Quantitative High-Throughput Screening with Large-Scale Tunable Gradients Based on a Microfluidic Droplet Robot under Unilateral Dispersion Mode

Yan Wei, Ying Zhu, and Qun Fang

Anal. Chem., **Just Accepted Manuscript** • DOI: 10.1021/acs.analchem.8b04564 • Publication Date (Web): 27 Feb 2019

Nanoliter Quantitative High-Throughput Screening with Large-Scale Tunable Gradients Based on a Microfluidic Droplet Robot under Unilateral Dispersion Mode

Yan Wei, Ying Zhu,*,† Qun Fang*

Institute of Microanalytical Systems, Department of Chemistry and Center for Chemistry of Novel & High-Performance Materials, Zhejiang University, Hangzhou, 310058, China

† Present address: Environmental Molecular Sciences Laboratory, Pacific Northwest National Laboratory, Richland, Washington 99354, United States

CORRESPONDING AUTHOR FOOTNOTE:

Qun Fang

Email: fangqun@zju.edu.cn

Ying Zhu

Email: yingzhu@zju.edu.cn

ABSTRACT Performing quantitative high throughput screening (qHTS) is in urgent need in current chemical, biological and medical researches. In this work, we developed an automated microfluidic dilution and large-scale screening system in the nanoliter range, by combining the droplet-based microfluidic robot technique with a novel unilateral Taylor-Aris dispersion-based dilution approach. The unilateral dispersion approach utilizes multiphase microfluidic design to generate concentration gradient with fast gradient generation time, low sample/reagent consumption, and high operation efficiency over the widely-used bilateral Taylor-Aris dispersion approach adopted in previous dilution systems. The present system is capable to automatically generate large and tunable range of concentration gradients covering ca. 6 orders of magnitude in droplet arrays, and to achieve qHTS of large number of different samples. We applied the microfluidic droplet system in miniaturized enzyme kinetic assay in 8-nL droplets, and high-throughput quantitative screening of enzyme inhibitors with a library of 102 compounds. Only 9.8 μL of enzyme solution was consumed in 2448 droplet assays containing 102 compounds and 24 concentrations, representing an approximate 1600-fold reduction compared with multiwell plate-based assays. In the screening, dose-response curves of each tested compounds were established and 4 hits (CP-471474, ilomastat, batimastat, and marimastat) were screened to have inhibitory activity to matrix metallopeptidase-9 (MMP-9), which demonstrated that the present system has the potential to provide a miniaturized qHTS platform for drug discovery.

Since its origin in drug discovery, high throughput screening (HTS) has undergone rapid progress and built one of the major foundations of current chemical and biological researches.[1] To improve screening accuracy and precision, in 2006, Inglese et al.[2] developed quantitative high throughput screening (qHTS) technique, by which assays were performed at multiple different compound concentrations spanning more than four orders of magnitude to generate dose-response curves for all tested compounds. The qHTS technique eliminated primary single-concentration screening step in traditional HTS, which was found to have high rates of false positives and false negatives.[3] Optimal concentration conditions or structure-activity relationships can be directly revealed in a single primary screening round under the qHTS mode. However, qHTS dramatically increased the assay numbers and thus the consumption of biological samples and reagents as well as the time and labor costs, posing challenges for resource-limited studies or routine laboratories. Thus, assay miniaturization is essential for the successful implementation and application of qHTS technique.

The emerging of microfluidics has provided a potential solution for qHTS technology by performing biochemical assays in microfabricated channels, chambers, or water-in-oil droplets, instead of microtiter plates.[4,5] The assay volumes of microfluidic are commonly in the range of picoliters to nanoliters,[6] representing over 1000-times reduction in qHTS cost. The miniaturization of assay scale further enabled a variety of new applications including the screening of biologically-interest but

scarce protein samples,[7] single cell cytotoxicity assay,[8] and protein evolution.[9]

The combination of droplet-based microfluidics with gradient generation modules provides an effective way to carry out qHTS in nanoliter scale.[7,10–13] In droplet-based microfluidic systems, picoliter-to-nanoliter droplets are generated in microfabricated structures and then compartmented by immiscible oil phase.[14] Droplets are generated in high throughput and each droplet serves as an independent reactor without cross contamination with others. To form concentration gradient in series of droplets, the most widely used method is based on the adjusting of the merging flow rate ratio of sample and diluent streams by pumps.[7] Because of the precision of the infusion pumps, the dilution ranges of this type of systems are limited to 2 orders of magnitude. To expand concentration range, a droplet system was developed by trapping a sample droplet in a microchamber, sequentially merging with blank droplets, and finally releasing a series of diluted droplets.[11] A concentration gradient spanning over 4 orders of magnitude was achieved. Another efficient approach to generate large gradient range in droplets is to use the Taylor-Aris dispersion of a sample plug in a continuous diluent flow. With this approach, longitudinal concentration gradients ranging 3-4 orders of magnitude could be formed in dispersion channels and finally compartmented into droplets.[12,13] Such an approach was further integrated with an autosampler to implement quantitative high throughput screening of hundreds of compounds against a protein target.[12] Droplet-based microfluidic techniques have successfully demonstrated their abilities in reducing screening cost and improving assay accuracy and precision. However, a common criticism to current microfluidic

systems is the lack of versatility and flexibility in system operation and application, as usually one microfluidic system was developed to solve one special problem.

Herein, we developed an automated and versatile microfluidic dilution system to implement nanoliter-scale quantitative high throughput screening to address these challenges. The system was developed by combing a droplet robot platform[6,15,16] with a novel unilateral dispersion approach. The droplet robot is capable to manipulate picoliter-to-nanoliter droplets on a microfabricated nanowell-array chip, and enables the automated screening and assay of hundreds of different samples by directly interfacing a commercial multiwell plate to the nanoliter droplet-array chip.[6,16] Differing from the frequently used bilateral dispersion mode used in previous Taylor-Aris dispersion-based dilution systems,[12,13] the unilateral dispersion approach was developed to generate concentration gradient in a sequence of droplets rapidly and efficiently. By simply changing the volumes of samples and diluents, the gradient profile could be tuned within ca. 6 orders of magnitude to meet the requirements of diverse biological assays and screenings. We demonstrated the versatility of the present system in enzyme kinetic assay and quantitative screening of enzyme inhibitors.

EXPERIMENTAL SECTION

Setup of the Microfluidic Droplet system. The droplet system was built mainly on the basis of our previous-reported droplet robot systems,[15,16,17] which was composed of a capillary probe with a tapered tip connected with a syringe pump

(PHD 2000, Harvard Apparatus, Holliston, MA), a nanowell array chip for loading droplet array, and a commercial 384-well plate for containing different samples and reagents. Both the nanowell array chip and the 384-well plate were installed on an automated x-y-z translation stage (PSA series, Zolix, Beijing, China). The movement of the translation stage and the liquid aspirating/depositing of the syringe pump were precisely controlled by a lab-written Labview program (Labview 8.0, National Instruments, Austin, TX). The tapered tip of the capillary probe (150-mm i.d., 250-mm o.d., Reafine Chromatography Co., Yongnian, China) was fabricated using the heating and pulling method as described previously[15] with a tip size of 40 ± 5 μm i.d. and 50 ± 5 μm o.d.. Before use, the capillary surface was coated with a hydrophobic reagent named Aquapel Glass Treatment (PPG Industries, Pittsburgh, PA).

The nanowell array chips were fabricated with glass substrates with chromium and photoresist coating (Shaoguang Microelectronics, Changsha, China) using standard photolithography and wet chemical etching techniques as described previously.[18] A poly(methyl methacrylate) (PMMA) frame with a thickness of 2 mm was glued on each microchip to form a shallow reservoir on the chip for containing the cover oil. The microchip has nanowell size of 65 μm in depth and 280 μm in diameter, and an interval distance between adjacent wells of 400 μm, corresponding to a capacity of 3025 wells. Before use, the chip was treated with 1% octadecyltrichlorosilane (OTCS, Sigma-Aldrich Co., St. Louis, MO) in isooctane (v/v) to make their surfaces hydrophobic. A stereomicroscope (SMZ850T, Touptek, Hangzhou, China) with a

CCD camera (HV3151UC, Daheng Imavision, Beijing, China) was used to monitor the entire operation for droplet generation.

Generation of Droplet Array with Concentration Gradients. Prior to use, the capillary was prefilled with water as carrier. Before aspirating sample or reagent solutions, the capillary probe aspirated 50 nL of Fluorinert oil (FC-40, 3M, St. Paul, MN) to isolate the carrier from the subsequently aspirated sample/reagent solutions. Formation of droplet concentration gradient included three steps (Figure 1a and 1b). First, the capillary probe was inserted into the sample solution loaded in the multiwell plate and aspirated a plug of the sample into the capillary channel. Second, the capillary probe was inserted into the diluent solution, and aspirated a diluent plug into the capillary, during which a longitudinal concentration gradient was generated along the capillary channel based on Taylor dispersion. Third, the capillary probe was switched to the nanowell array chip, and sequentially deposited the dispersed sample plug into a series of nanowells to generate a droplet array with a concentration gradient. The flow rate in the syringe pump was set at 300 nL/min unless stated otherwise. During the experiment, a mineral oil layer with a thickness of ~1.5 mm was covered on the microchip to prevent droplet evaporation.

Calibration of in-Droplet Concentrations. The concentrations of the gradient droplet array formed by the droplet dilution system was calibrated using the relative time-based method previously described.[13] A fluorescent dye with a similar molecular weight to the tested samples was chosen as the standard for concentration calibration. Thus, sodium fluorescein (376 Da) was used as the standard in enzyme kinetic

measurement and enzyme inhibitor screening. A series of droplets of the fluorescent standard solutions in the concentration range of 1 nM – 2 mM were sequentially formed and their fluorescence intensities were measured by an inverted fluorescence microscope (Nikon Eclipse TE-2000-S, Nikon, Japan) to build standard curves between the in-droplet standard concentration and droplet fluorescence intensity. By adjusting the exposure parameters of the fluorescence microscope, a detectable concentration range of 6 orders of magnitude for fluorescein was achieved with a detection limit of 1 nM. Then, 1 mM fluorescent standard solution and diluent were sequentially introduced into the capillary probe and a droplet array with the standard's concentration gradient was formed on the nanowell chip with the same operation conditions as the assay for actual samples. The concentration of each droplet in the droplet gradient was obtained using the standard curves. Based on these results, a relationship between the droplet sequence number and the dilution factor (ratio of the initial standard concentration to droplet concentration) was obtained, with which we could calibrate the concentrations of analytes in the droplet gradients formed in actual sample assays under the same conditions as the standard including the capillary probe, introduced sample and diluent volumes, and aspirating flow rate.

Enzyme Kinetic Measurement. All solutions for the enzyme assay were freshly prepared. Matrix metallopeptidase-9 (MMP-9, R&D Systems, Minneapolis, MN) and MMP substrate III (substrate, AnaSpec, Fremont, CA) solutions were prepared with the reaction buffer (150 mM NaCl, 50 mM Tris, 10 mM $CaCl_2$, 0.05% Tween-20, 0.05% Brij-35, and 0.1% BSA at pH 7.5). For performing the enzyme kinetic

measurement, an array of 4-nL droplets with substrate concentration gradients was first formed by introducing 30 nL of 600 μM substrate solution and 50 nL of reaction buffer into the capillary probe. Twenty droplets were generated in one gradient droplet array, among which the first and the last droplets were discarded by depositing them into the waste well instead of the microchip. After the generation of the substrate droplet array, the capillary probe was washed with 100 nL of the reaction buffer to reduce cross contamination. Then, 4 nL of 40 nM enzyme solution was added to each droplet by the capillary probe under the semi-contact depositing mode.[16] Finally, the microchip with the reaction droplet array was heated to 37 °C with a homemade heater to initiate the in-droplet enzymatic reactions. The fluorescence intensity of the droplets array was continuously measured by a homemade fluorescence detector[19] (480 nm/529 nm excitation/emission wavelengths, 7.6 mm × 7.6 mm view field) every 8 min for 40 min. We chose 15 droplets (droplet sequence No. 2–16) with concentration range within three orders of magnitude for the kinetic measurement.

Enzyme Inhibitor Screening. The enzyme inhibitor screening was performed with a similar procedure to the MMP-9 kinetic measurement. A chemical library including 100 compounds (10 mM) in DMSO was purchased from Selleck Chemicals (Houston, TX). Stock solutions of two known inhibitors of MMP-9, marimastat and CP471474 (Sigma-Aldrich Co., St. Louis, MO), were prepared with concentration of 10 mM in DMSO. Before use, the concentrations of the stock solutions of the tested compounds were diluted to 1 μM with the reaction buffer. A large-scale droplet array containing

concentration gradient droplets (4 nL) of all tested compounds was first generated on the microchip with an introduce volume of 50 nL for both the sample and reaction buffer. Then, 4 nL of 15 nM enzyme solution and 4 nL of 66.45 μM substrate solution were sequentially added into each compound droplet to reach a final droplet volume of 12 nL. The time for forming the gradient droplet array of the whole 102 tested compounds was 120 min. The time required for adding the enzyme and substrate into the 2448 droplets were ca. 60 and 60 min, respectively. To prevent sample and reagent evaporation, 0.2 mL of mineral oil was added into each well of the multiwell plate during the entire droplet manipulation process. The reaction droplet array was heated to 37 °C on the heater to trigger the reaction and detected by the fluorescence detector after 72-min incubation.

RESULTS AND DISCUSSION

System Design and Operation. The main objective of this work is to develop an automated droplet dilution system capable of providing tunable concentration gradients over large orders of magnitude for performing quantitative high throughput screening and miniaturized biochemical assays with nanoliter-scale sample consumptions. The droplet system was built mainly on the basis of a liquid-handling robot using a capillary probe connected with a syringe pump to couple with a microfabricated nanowell-array chip and a multiwell plate installed on an automated 3-dimensional translation stage (Figure 1a).[6,15,16] To meet the requirement of qHTS with 10-fold higher assay numbers than the routine screenings,[2] ultrahigh density

nanowell-array chips were fabricated using the photolithography technique with 3025 nanowells produced on a 2.2 cm × 2.2 cm region of the chip (Figure 1c).

In traditional concentration gradient generation systems as well as microfluidic systems based on Taylor-Aris dispersion, bilateral dispersion (Figure 2a1) is the only and routine mode used for generating gradient. In this method, a sample plug is injected into a continuously-flowing diluent stream and mixes with the bilateral diluents in the formed diluent-sample-diluent stream, producing a peak-shaped concentration gradient profile. By combining the droplet-based microfluidic robot technique with the Taylor-Aris dispersion-based gradient generation technique, we developed the unilateral dispersion approach to generate concentration gradient by limiting the dispersion of sample plug to only one side using an immiscible oil (Figure 2a2). Under the unilateral dispersion mode, a gradient droplet array was formed by sequentially aspirating plugs of the oil, sample and diluent solutions into the capillary probe to form an oil-sample-diluent stream, then delivering the mixed aqueous solutions out and depositing them into nanowells to generate a sequence of droplets with concentration gradient (Figure 1b). During the aspirating and delivering processes, the sample and diluent plugs in the oil-sample-diluent stream mixed with each other in the capillary channel based on Taylor dispersion and produced a longitudinal concentration gradient along the capillary. However, in the other side of the oil-sample-diluent stream, no sample dispersion occurred due to the use of the immiscible oil instead of the diluent (Figure 2a2).

Comparing with the conventional gradient systems based on the bilateral

dispersion mode, the present unilateral dispersion-based system has five features as follows. (1) It allows to generate similar scope of concentration gradient but with less than 50% of droplet number, gradient generation time and reagent consumption (Figure 2b and 2c). This leads to a more than 2-fold increase in screening throughput. (2) The unilateral dispersion-based gradient droplet forming operation is composed by three simple steps including aspirating sample, aspirating diluent and depositing droplets by the capillary probe (Figure 1b). Such a capillary-based operation is easy to be performed automatically and allows convenient sample change among different samples, which makes the system especially suitable for screening a large number of different samples in qHTS. (3) The range of the in-droplet concentration gradient can be flexibly tuned from 1 to ca. 6 orders of magnitude by simply changing the volume ratio of the aspirated sample and diluent solutions. This endows the dilutor wide applicability for different types of applications. (4) High efficient and fast dispersion can be achieved between the nanoliter-scale sample and diluent plugs in the capillary channel with a length of a few millimeters by the aspirating-depositing operation, which leads to much fewer numbers of droplets than other systems with the same gradient range. For example, in the present system, 25 droplets could be formed in 70 s with a gradient range of 5.5 orders of magnitude, while more than double number of droplets in the comparison experiment (Figure 2b), more than 240 droplets in a microchip-based gradient system[13] or ca. 10,000 droplets in a capillary-microchip based gradient system,[12] were used to obtain the similar gradient range. This feature significantly improves the droplet utilization efficiency and thus the working

efficiency of the droplet system. (5) Under the unilateral dispersion mode, the operation conditions that can mainly affect the gradient performance only includes the sample volume, diluent volume, and flow rate, all three of which could be precisely controlled by the liquid handling module of the present system. Therefore, good generation reproducibility and working reliability can be obtained (see "Tunable Droplet Dilution System" part for details), which is essential for a qHTS system facing a large number of samples.

In the present system, the static droplet array format was used that allows each droplet in the array can be indexed by its position, and individually manipulated and detected on demand.[15-17] Compared with continuous-flow droplet systems,[12,13,20] such a format is beneficial for biological assays requiring time-lapse detection and long-term incubation, such as kinetic assays and protein crystallization screenings.

Tunable Droplet Dilution System. The concentration gradient profile formed by the droplet dilution system could be simply tuned by adjusting the sample/diluent volume ratio and the flow rate of the syringe pump without changing the system setup. We evaluated the effects of these parameters on the gradient profile using fluorescein as a model sample (Figure 3a-c). By changing the sample volumes in the range of 5-70 nL with a fixed diluent volume of 50 nL, similar gradient profiles with different droplet numbers and gradient ranges were observed (Figure 3a). With the increase of the sample volume, the droplet number and gradient range increased. When the sample volume was larger than 30 nL, 5.5 orders of magnitude of concentration gradient could be obtained. Further increase of the sample volume was unfavorable as

it only increased the number of droplets with similar concentrations.

With a fixed sample volume of 50 nL, the diluent volume exhibited significant affect in the gradient profile in the range of 10-70 nL (Figure 3b). The gradient ranges were increased from 0.4 to 5.5 orders of magnitude with the increase of the diluent volume from 10 to 50 nL. Such a property could be used to flexibly adjust the gradient range by simply changing the diluent volume. In the present work, the further extending of the gradient range to dilution factors was limited by the sensitivity of the fluorescence detector, as indicated by the three undetectable droplets (droplet sequence No. 2, 3, and 4 in Figure 3b) with the diluent volume of 70 nL.

Compared with the diluent volume, the flow rate of the syringe pump (i.e. the flow rates of aspirating sample/diluent solution and depositing dispersed stream) have contrary effect on the gradient range in the range of 50-900 nL/min. As shown in Figure 3c, larger gradient ranges were obtained at lower flow rates. Although relatively low flow rates were beneficial for gradient generation, they also proportionally increased the experimental time and thus reduced the screening throughput. The flow rate of 300 nL/min appeared to be a good comprise between the gradient generation and experimental throughput.

We also tested the effect of the gradient generation time on the gradient profile by using different droplet generation time intervals of 0.5 s and 2.0 s (i.e. time interval between generating two adjacent droplets). The results (Figure S1) show that no obvious influence in the gradient profile was observed by increasing the time interval from 0.5 s to 2.0 s. In addition, the present system has the ability to precisely control

the operation time with precision within 1 ms, which ensure a good reproducibility in the time of gradient generation.

Finally, it is crucial to select proper fluorescent calibration standards to match the tested samples, as molecular weight (MW) could also affect the gradient profile. Figure 3D shows the effect of the sample molecular weight on gradient profile using four standards with different molecular weights, sodium fluorescein (376 Da), FD4 (ca. 4,000 Da), FD10S (ca. 10,000 Da), and FD70 (ca. 70,000 Da). With the increase of the molecular weight, the corresponding gradient range decreased. Such a phenomenon could be explained by the Taylor dispersion on the basis of the convective diffusion and molecular diffusion of the sample molecules.[12,21] For low-molecular-weight samples, their molecular diffusion effects contributed to dispersion are stronger than those of high-molecular-weight samples, resulting in relatively large gradient range. This result implies that a standard with similar molecular weight to tested samples should be used in the calibration of in-droplet concentrations.

Based on the above experiments, the present dilution system could be optimized to meet the requirement of diverse applications by tuning the experimental parameters.

Measurement of Enzyme Kinetics. Enzyme kinetics, involving the measurements of the rates of enzyme-catalyzed reactions, is crucial to reveal catalytic mechanism and metabolic pathways in biochemical systems. As two of well-known enzyme kinetic parameters, Michaelis-Menten constant (K_m) and maximum reaction rate (V_{max})[22] are usually measured by monitoring the reaction rates with increased

substrate concentrations. Here, the present system was applied to measure the Michaelis-Menten kinetic parameters with nanoliter-scale enzyme and substrate consumptions by generating a series of substrate droplets with a concentration gradient. Considering 2-3 order-of-magnitude dilution of substrate was required, we set the sample and diluent volumes as 30 nL and 50 nL, respectively, and selected 15 droplets with dilution factors below 334. MMP-9 and MMP substrate III were used as the model system for the measurement. In the enzymatic reaction, MMP-9 catalyzes the hydrolytic cleavage of a fluorogenic peptide substrate, liberating the fluorophore (FAM) and the quencher (QXL520), thus yielding detectable fluorescent signals. We monitored the reaction process for 40 min and recorded the fluorescence images of droplets every 8 min. As shown in Figure 4a, the droplet fluorescence intensity increased with both reaction time and substrate concentration. Triplicate experiments further confirmed the reaction rate increased with the substrate concentration (Figure 4b). As the concentration of FAM had a linear correlation with the fluorescence intensity (Figure 4c), reaction rate could be calculated and a Michaelis-Menten equation plot could be built (Figure 4d). The half-maximal activity (Michaelis-Menten constant, K_m) and the turnover number (K_{cat}) of MMP were 16.9 ± 2.0 μM and 8.2 ± 0.2 /min, respectively, which are close to the results (8.1 ± 1.1 μM and 14.1 ± 0.9 /min) previously reported using microliter plates with the same pro-fluorescent substrate.[23]

Quantitative High Throughput Inhibition Screening of MMP-9. It is well-known that the biological effect of a compound is depending on both its

chemical structure and concentrations.[24] For example, half maximal inhibitory concentration (IC_{50}) is used to evaluate the effectiveness of a compound in inhibiting a specific biological function. Far below an IC_{50}, no evident effect can be observed, and on the contrary, far over it, side or "toxic" effects may be observed.[25]

A commercial Cherry Pick Library containing 100 compounds (86 of them are FDA-approved) and 2 known MMP-9 inhibitors[26] (Table S1) were screened for the inhibition of MMP-9, a target reported associated with cancer metastasis.[27,28] The droplet system was employed to generate large-scale concentration gradients spanning 5.5 orders of magnitude by setting both sample and diluent volumes as 50 nL. For each compound, 24 droplets were generated with a volume of 4 nL for each droplet (only the first droplet was discarded in this screening experiment), thus total 2448 screening assays were performed for 102 compounds (Figure 5 and Figure S2). All the 2448 assays were successfully implemented, demonstrating high robustness of the nanoliter screening system. The screening revealed 4 compounds with inhibition activity including two known inhibitors (No. 10 CP-471474 and No. 74 Marimastat) and two compounds (No. 23 Ilomastat and No. 55 Batimastat) newly reported with inhibitory action to MMPs[29,30]. Their IC_{50} values calculated based on Sigmoidal fitting method were 8.4 nM (No. 10), 0.60 nM (No. 23), 0.32 nM (No. 55), and 5.1 nM (No. 74), respectively. A repeated screening further confirmed the results with IC_{50} values of 11.5 nM (No. 10), 0.7 nM (No. 23), 0.5 nM (No. 55), and 4.5 nM (No. 74), respectively (Figure S3). The measured values for two known MMP-9 inhibitors were also agreed well with the results reported in previous studies (11.9 nM for No.10

and 3.2 nM for No. 74) using different approach.[26]

Although qHTS can effectively address the challenges of conventional HTS in reducing false positives and false negatives,[2,31,32] its broad dissemination is hindered by large sample/reagent consumption and low assay throughput. Performing miniaturized qHTS in a microfluidic droplet system could provide the substantial possibility for significantly reducing the screening consumption to nanoliter samples or reagents for each trial, and achieving large-scale and high-throughput screening with over thousand assays. As demonstrated in the enzyme inhibition screening, total 9.8 μL MMP-9 enzyme solution was consumed in 2448 droplet assays containing 102 compounds and 24 concentrations, which represented an approximate 1600-fold reduction compared with 8-point multiwell plate-based assays (20 μL for each assay). The current screening throughput was 70 s per compound, corresponding to 1234 samples per day (24 h). Furthermore, the screening throughput could be increased linearly by using multiple sampling probes to achieve > 10,000 samples per day. The high density and compact structure of the nanowell chips also facilitate the accommodation of large-number of microreactors and the readout of massive data.

CONCLUSIONS

The present droplet system provides a versatile, robust, fully-automated liquid handling platform for nanoliter-scale chemical and biological assays. It enabled rapid and programmable sample/reagent dilutions with high dynamic ranges of ca. 6 orders of magnitude. Compared with traditional serial dilution approach requiring more than 10 pipetting steps, the present approach significantly simplified the serial dilution

operation to only three steps (Figure 1b). Compared with other microfluidic dilution approaches,[11,13,20,23,33] the droplet system addressed the challenge of world-to-chip interface[34] as it was built on the basis of a robotic system and could directly access to large number of different samples and reagents filled in multiwell plates. The present system can be readily embedded into an existing high throughput liquid handling system without substantial modification of hardware. As droplet reactions were performed within nanowells fabricated on glass microchips with excellent optical transparency, the present platform is compatible with majority biological assays using detection methods of fluorescence or bright-filed imaging. In addition to the fluorescence imaging method employed in the present work, other detection methods such as high-sensitive label-free mass spectrometry,[35,36] high-resolution liquid chromatography or capillary electrophoresis,[37,38] could be used for the measurement of droplets.

When a droplet-based microfluidic system is applied in high throughput screening with a large number of different tested compounds, there is a potential risk of the uncontrollable partitioning of some highly hydrophobic components in the droplets into the carrier (cover) oil phase, which may lead to cross contamination and limit its broad application of this technology in high throughput screening with a large number of different tested compounds. This problem could be solved by fabricating independent chambers on the chip for loading individual cover oil and droplet to completely eliminate the possibility of cross-contamination between different droplets, or by controlling the ambient humidity within the system to suppress the evaporation

of droplets without the use of oil phase.

In this work, the present droplet system was applied in molecular drug screening with ca. 6 orders of magnitude concentration gradient for tested compounds. In addition to the molecular level screening, the similar gradient forming method could also be adopted in cell-based screening by automatically adding the gradient droplets of tested compounds into preformed droplets culturing cells.[39] The use of large scale of compound concentration scope will significantly improve screening throughput, reduce sample/reagent consumption, and provide more information for cellular screening.

Acknowledgment

Financial supports from Natural Science Foundation of China (Grants 21435004, 21475117, and 21227007), and Natural Science Foundation of Zhejiang Province (Grant LY14B050001) are gratefully acknowledged.

Supporting Information Available

Supporting information as noted in the text is available free of charge via http://pubs.acs.org.

REFERENCE

(1) Pereira, D. A.; Williams, J. A. *Br. J. Pharmacol.* **2007**, *152*, 53–61.

(2) Inglese, J.; Auld, D. S.; Jadhav, A.; Johnson, R. L.; Simeonov, A.; Yasgar, A.; Zheng, W.; Austin, C. P. *Proc. Natl. Acad. Sci.* **2006**, *103*, 11473–11478.

(3) Malo, N.; Hanley, J. A.; Cerquozzi, S.; Pelletier, J.; Nadon, R. *Nat. Biotechnol.* **2006**, *24*, 167–175.

(4) Whitesides, G. M. *Nature* **2006**, *442*, 368–373.

(5) Sackmann, E. K.; Fulton, A. L.; Beebe, D. J. *Nature* **2014**, *507*, 181–189.

(6) Liu, W. W.; Zhu, Y.; Fang, Q. *Anal. Chem.* **2017**, *89*, 6678–6685.

(7) Li, L.; Mustafi, D.; Fu, Q.; Tereshko, V.; Chen, D. L.; Tice, J. D.; Ismagilov, R. F. *Proc. Natl. Acad. Sci.* **2006**, *103*, 19243–19248.

(8) Brouzes, E.; Medkova, M.; Savenelli, N.; Marran, D.; Twardowski, M.; Hutchison, J. B.; Rothberg, J. M.; Link, D. R.; Perrimon, N.; Samuels, M. L. *Proc. Natl. Acad. Sci.* **2009**, *106*, 14195–14200.

(9) Agresti, J. J.; Antipov, E.; Abate, A. R.; Ahn, K.; Rowat, A. C.; Baret, J.-C.; Marquez, M.; Klibanov, A. M.; Griffiths, A. D.; Weitz, D. A. *Proc. Natl. Acad. Sci.* **2010**, *107*, 4004–4009.

(10) Theberge, A. B.; Whyte, G.; Huck, W. T. S. *Anal. Chem.* **2010**, *82*, 3449–3453.

(11) Niu, X.; Gielen, F.; Edel, J. B.; DeMello, A. J. *Nat. Chem.* **2011**, *3*, 437–442.

(12) Miller, O. J.; Harrak, A. E.; Mangeat, T.; Baret, J. -C.; Frenz, L.; Debs, B. E.; Mayot, E.; Samuels, M. L.; Rooney, E. K.; Dieu, P.; Galvan, M.; Link, D. R.; Griffiths, A. D. *Proc. Natl. Acad. Sci.* **2012**, *109*, 378–83.

(13) Cai, L. F.; Zhu, Y.; Du, G. S.; Fang, Q. *Anal. Chem.* **2012**, *84*, 446–452.

(14) Teh, S.-Y.; Lin, R.; Hung, L.-H.; Lee, A. P. *Lab Chip* **2008**, *8*, 198–220.

(15) Zhu, Y.; Zhang, Y. X.; Cai, L. F.; Fang, Q. *Anal. Chem.* **2013**, *85*, 6723–6731.

(16) Zhu, Y.; Zhu, L.-N.; Guo, R.; Cui, H.-J.; Ye, S.; Fang, Q. *Sci. Rep.* **2014**, *4*, 5046.

(17) Zhu, Y.; Zhang, Y.-X.; Liu, W.-W.; Ma, Y.; Fang, Q.; Yao, B. *Sci. Rep.* **2015**, *5*, 9551.

(18) Fang, Q.; Xu, G. M.; Fang, Z. L. *Anal. Chem.* **2002**, *74*, 1223–1231.

(19) Yu, Z.; Zhu, Y.; Zhang, Y.; Li, J.; Fang, Q.; Xi, J.; Yao, B. *Talanta* **2011**, *85*, 1760–1765.

(20) Baccouche, A. Okumura, S.; Sieskind, R.; Henry, E.; Aubert-Kato, N.; Bredeche, N.; Bartolo, J.-F.; Taly, V.; Rondelez, Y.; Fujii, T.; Genot, A. J. *Nat. Protoc.* **2017**, *12*, 1912–1932.

(21) Du, W.-B.; Fang, Q.; Fang, Z.-L. *Anal. Chem.* **2006**, *78*, 6404–6410.

(22) Walter, N. G. *Nat. Chem. Biol.* **2006**, *2*, 66–67.

(23) Jambovane, S.; Kim, D. J.; Duin, E. C.; Kim, S. K.; Hong, J. W. *Anal. Chem.* **2011**, *83*, 3358–3364.

(24) Hill, A. V. *J. Physiol.* **1910**, *40*, 4–7.

(25) Kenakin, T. *Nat. Rev. Drug Discov.* **2003**, *2*, 429–438.

(26) Yun, J. Y.; Jambovane, S.; Kim, S.-K.; Cho, S.-H.; Duin, E. C.; Hong, J. W. *Anal. Chem.* **2011**, *83*, 6148–6153.

(27) Bjorklund, M.; Koivunen, E. *Biochim. Biophys. Acta-Rev. Cancer* **2005**, *1755*, 37–69.

(28) Bendrik, C.; Robertson, J.; Gauldie, J.; Dabrosin, C. *Cancer Res.* **2008**, *68*, 3405–3412.

(29) Walz, W.; Cayabyab, F. S. *Neurochem. Res.* **2017**, *42*, 2560-2565.

(30) Zhang, X.; Bresee, J.; Fields, G. B.; Edwards, W. B. *Bioorg. Med. Chem. Lett.* **2014**, *24*, 3786-3790.

(31) Xia, M.; Huang, R.; Witt, K. L.; Southall, N.; Fostel, J.; Cho, M.-H.; Jadhav, A.; Smith, C. S.; Inglese, J.; Portier, C. J.; Tice, R. R.; Austin, C. P. *Environ. Health Perspect.* **2008**, *116*, 284–291.

(32) Shukla, S. J.; Huang, R.; Austin, C. P.; Xia, M. *Drug Discov. Today* **2010**, *15*, 997–1007.

(33) Dertinger, S. K. W.; Chiu, D. T.; Noo Li Jeon; Whitesides, G. M. *Anal. Chem.* **2001**, *73*, 1240–1246.

(34) Liu, J.; Hansen, C.; Quake, S. R. *Anal. Chem.* **2003**, *75*, 4718–4723.

(35) Sun, S.; Slaney, T. R.; Kennedy, R. T. *Anal. Chem.* **2012**, *84*, 5794-5800.

(36) Jin, D.; Zhu, Y.; Fang, Q. *Anal. Chem.* **2014**, *86*, 10796-10803.

(37) Fang, X. X.; Fang, P.; Pan, J. Z.; Fang, Q. *Electrophoresis* **2016**, *37*, 2376-2383.

(38) Ochoa, A.; Álvarez-Bohórquez, E.; Castillero, E.; Olguin, L. F. *Anal. Chem.* **2017**, *89*, 4889-4896.

(39) Du, G.; Pan, J.; Zhao, S.; Zhu, Y.; den Toonder, J. M. J.; Fang, Q. *Anal. Chem.* **2013**, *85*, 6740-6747.

FIGURE CAPTIONS

Figure 1. System setup and working principle. (a) Schematic diagram of setup of the microfluidic droplet gradient system (not to scale). (b) Three-step procedures for generating concentration gradient in a sequence of droplets. (c) A photography and enlarged microscopic image showing droplet array with concentration gradients formed by the droplet system. Seven different food dyes were used for the visualization of concentration gradients. The nanowell-array chip contains 3025 nanowells. Droplet volume: 4 nL.

Figure 2. (a) Comparison of conventional bilateral dispersion approach with the present unilateral dispersion approach. Two schematic diagrams show the principles of the bilateral dispersion (a1) and unilateral dispersion (a2). (b, c) Typical gradient profiles shown as the relationships of fluorescein concentration *vs.* droplet sequence number (b) and log dilution factor *vs.* droplet sequence number (c), generated under the bilateral dispersion mode by aspirating 1000 nL diluent, 50 nL sample and 50 nL diluent, and under the unilateral dispersion mode by aspirating 50 nL sample and 50 nL diluent. Droplet volume: 4 nL. Pump flow rate: 300 nL/min.

Figure 3. Evaluation and optimization of the droplet dilution system. (a) Effect of introduced sample volumes and (b) diluent volumes on the gradient profiles. (c) Effect of flow rates by fixing sample and diluent volumes both at 50 nL. Sodium fluorescein (1 mM) was used as a model sample in (a–c). (d) Effect of molecular weights on sample dispersion. Concentrations of the four fluorescent dyes, 0.1 mM; droplet volume, 4 nL; flow rate, 300 nL/min.

Figure 4. Measurement of enzyme kinetic parameters. (a) Typical time-lapse fluorescence images showing the in-droplet enzymatic reaction process. Substrate concentrations were generated by aspirating 30 nL of 600 μM MMP substrate III and 50 nL of diluent into the capillary, and then depositing the substrate-dispersed flow into the nanowells to generate gradient droplets with a volume of 4 nL for each droplet. The reaction droplets were formed by dispensing 4 nL, of 40 nM MMP-9 into each substrate droplet. Scale bar: 400 μm. (b) Fluorescence intensities of the droplets during the reaction process. (c) Standard curve of FAM concentration *vs* fluorescence intensity. (d) Michaelis-Menten equation curve transformed from (b) and (c). Standard deviations were obtained from triplicate measurements.

Figure 5. Quantitative high throughput inhibition screening of MMP-9. (a) Fluorescence images showing the total 2448 assay droplets for 102 tested compounds with 24 concentrations for each compound. Conditions for each assay: compound volume, 50 nL; diluent volume, 50 nL; gradient droplet number, 24; gradient droplet volume, 4 nL; volume of MMP-9 solution added into each gradient droplet, 4 nL; volume of substrate solution added into each gradient droplet, 4 nL. (b) Dose-response curves obtained from the results shown in (a), which reveals 4 compounds (No. 10, 23, 55, and 74) with inhibition activity (high-lighted with blue background). (c) Molecular structures of the hits obtained in the screening.

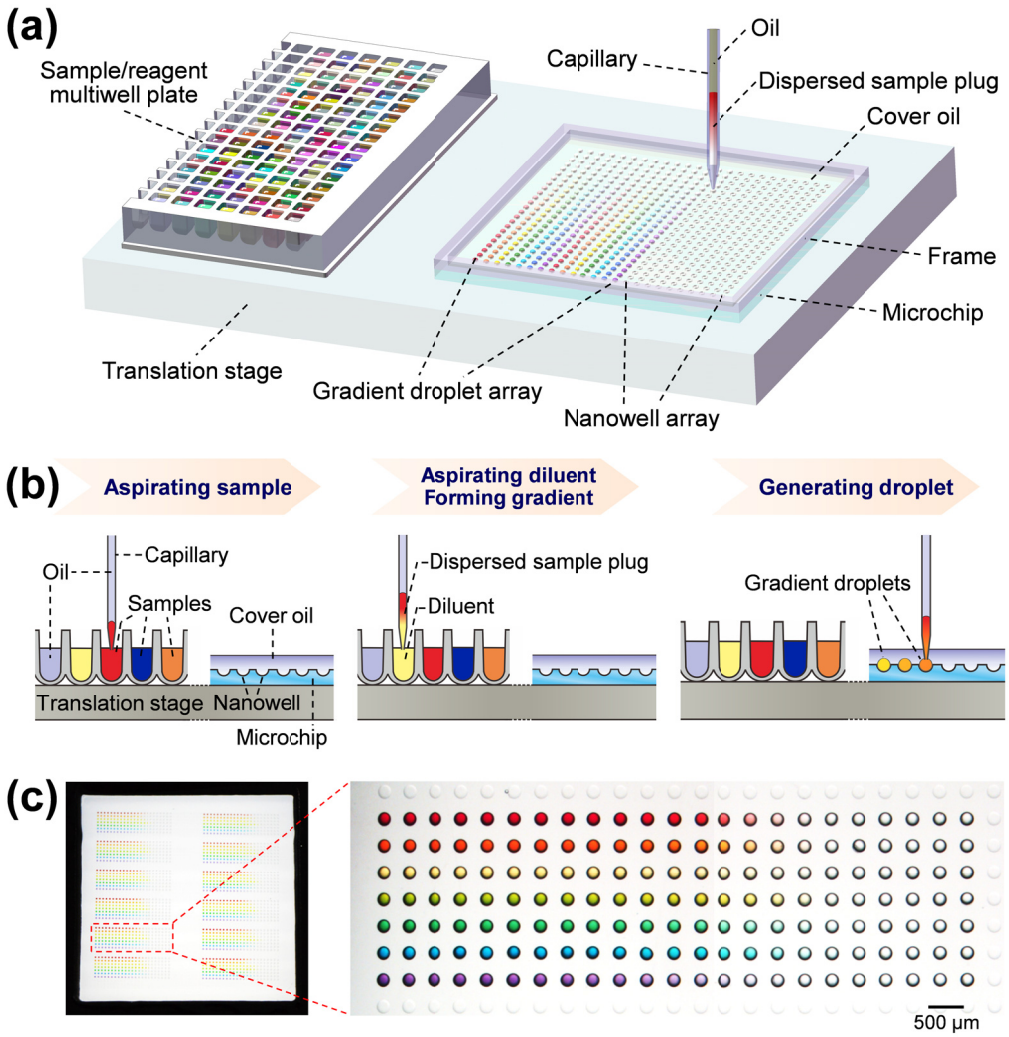
(a)
Sample/reagent multiwell plate
Capillary
Oil
Dispersed sample plug
Cover oil
Frame
Microchip
Translation stage
Gradient droplet array
Nanowell array
(b)
Aspirating sample
Aspirating diluent Forming gradient
Generating droplet
Oil
Capillary
Samples
Cover oil
Translation stage
Nanowell
Microchip
Dispersed sample plug
Diluent
Gradient droplets
(c)
500 μm

Figure 1

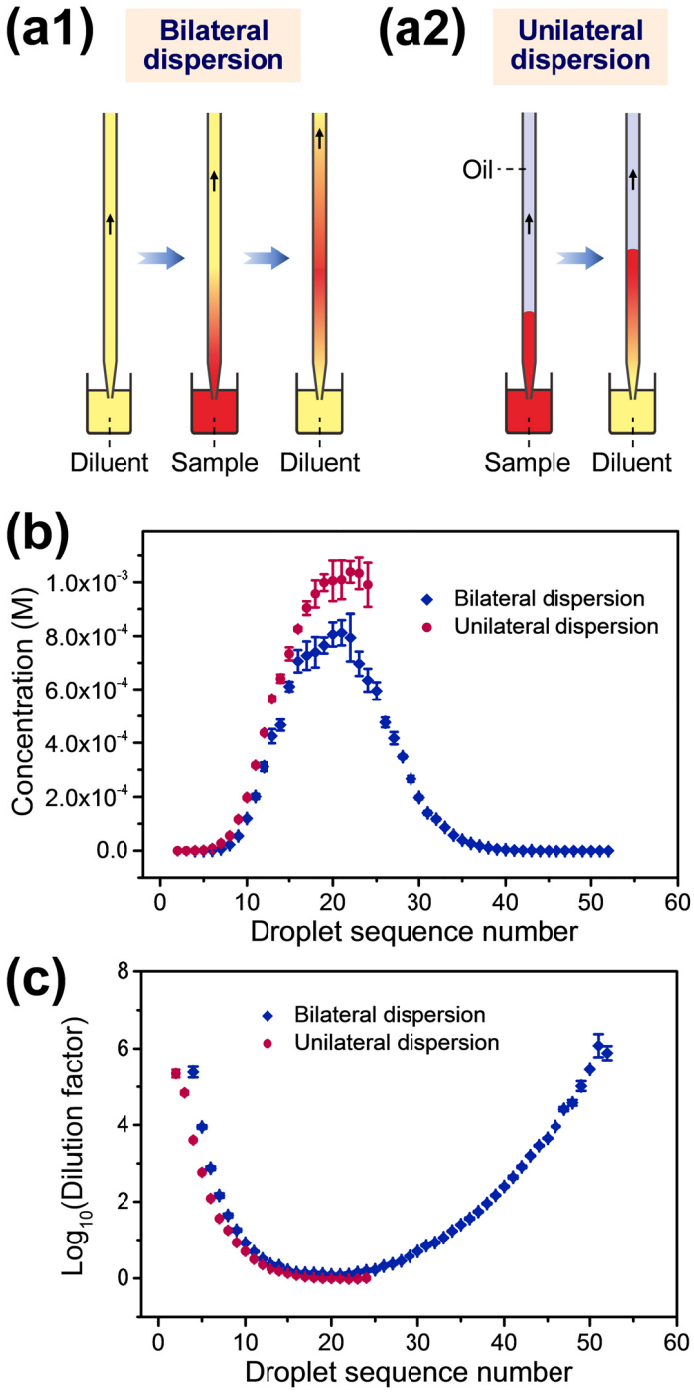
(a1)
Bilateral dispersion
(a2)
Unilateral dispersion
Oil
Diluent
Sample
Diluent
Sample
Diluent
(b)
Concentration (M)
1.0x10-3
8.0x10-4
6.0x10-4
4.0x10-4
2.0x10-4
0.0
0
10
20
30
40
50
60
Droplet sequence number
Bilateral dispersion
Unilateral dispersion
(c)
Log10(Dilution factor)
8
6
4
2
0
0
10
20
30
40
50
60
Droplet sequence number
Bilateral dispersion
Unilateral dispersion

Figure 2

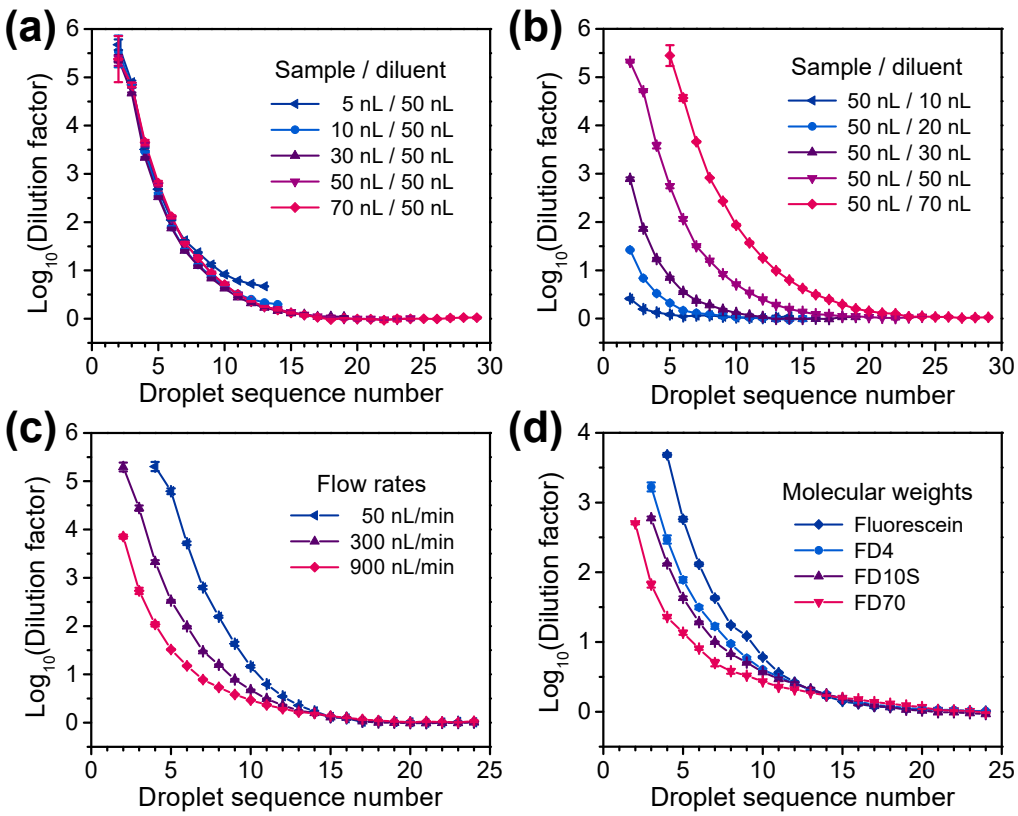
(a)
Log10(Dilution factor)
Droplet sequence number
Sample / diluent
5 nL / 50 nL
10 nL / 50 nL
30 nL / 50 nL
50 nL / 50 nL
70 nL / 50 nL
(b)
Log10(Dilution factor)
Droplet sequence number
Sample / diluent
50 nL / 10 nL
50 nL / 20 nL
50 nL / 30 nL
50 nL / 50 nL
50 nL / 70 nL
(c)
Log10(Dilution factor)
Droplet sequence number
Flow rates
50 nL/min
300 nL/min
900 nL/min
(d)
Log10(Dilution factor)
Droplet sequence number
Molecular weights
Fluorescein
FD4
FD10S
FD70

Figure 3

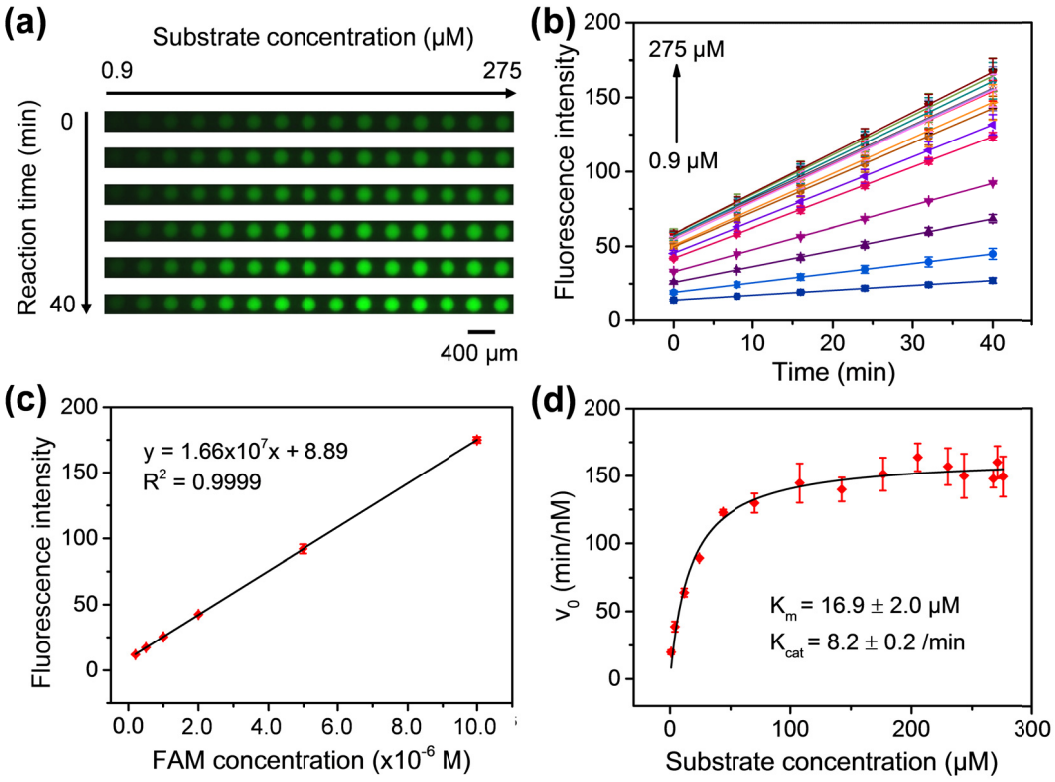
(a)
Substrate concentration (μM)
0.9
275
Reaction time (min)
0
40
400 μm
(b)
275 μM
0.9 μM
Fluorescence intensity
Time (min)
(c)
y = 1.66x10^7x + 8.89
R^2 = 0.9999
Fluorescence intensity
FAM concentration (x10^-6 M)
(d)
K_m = 16.9 ± 2.0 μM
K_cat = 8.2 ± 0.2 /min
v_0 (min/nM)
Substrate concentration (μM)

Figure 4

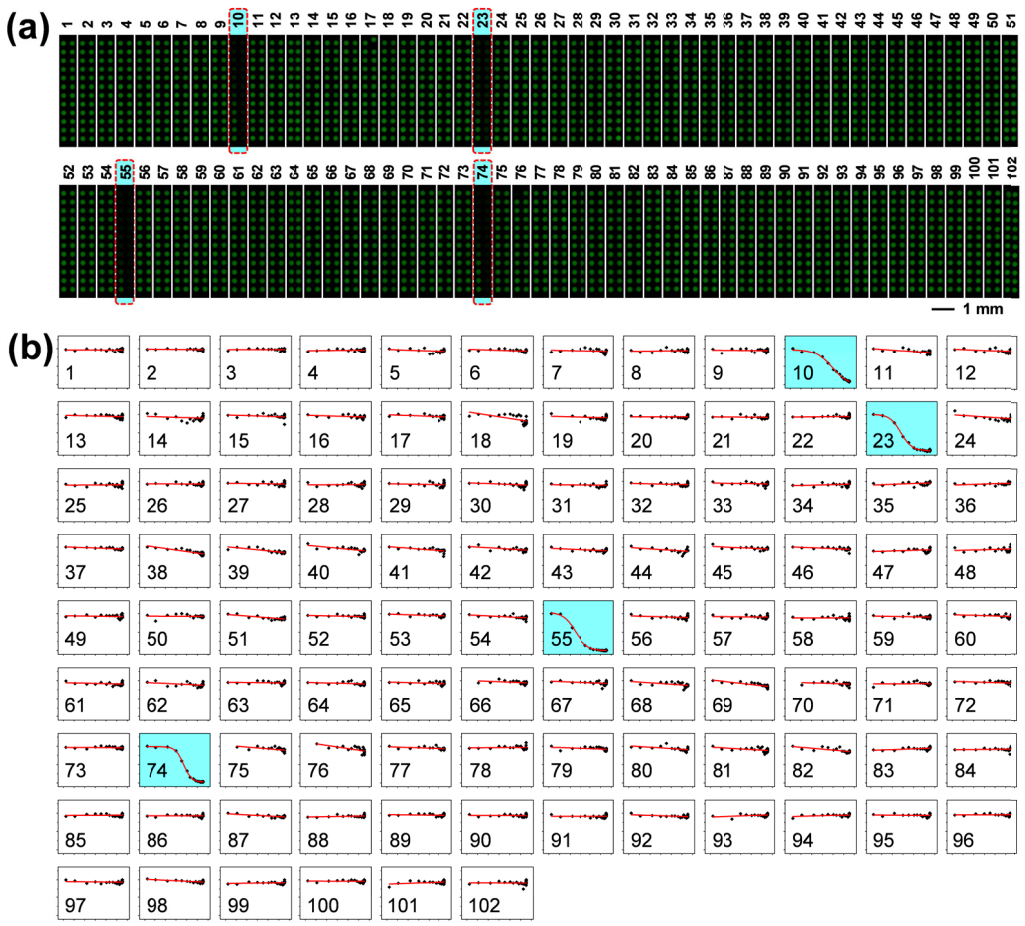
(a)
1 mm
(b)
(c)
No. 10 CP-471474
No. 23 Ilomastat
No. 55 Batimastat
No. 74 Marimastat

Figure 5

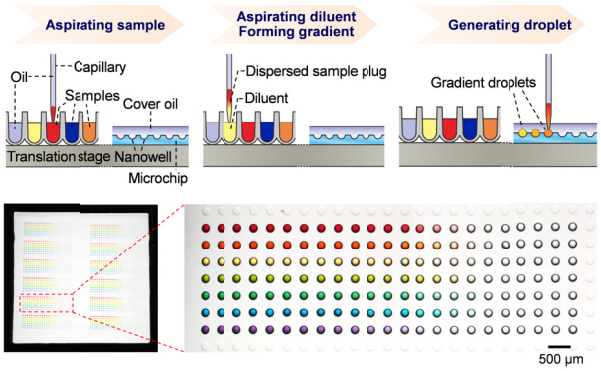
Aspirating sample
Aspirating diluent
Forming gradient
Generating droplet
Oil
Capillary
Samples
Cover oil
Translation stage
Nanowell
Microchip
Dispersed sample plug
Diluent
Gradient droplets
500 μm

TOC